Kimberlite (U-Th)/He dating links surface erosion with lithospheric heating, thinning and metasomatism in the southern African Plateau

Jessica R. Stanley, Rebecca M. Flowers, and David R. Bell

DATA REPOSITORY

(U-TH)/He ANALYTICAL METHODS

We acquired He dates for 24 aliquots of apatites from four samples (Table DR1). These included 10 single-grain apatites from the kimberlite matrix from the Uintjiesberg, Markt and Melton Wold kimberlites, and 10 single-grain apatites from crustal clasts consisting mostly of gneissic basement from Markt and Uintjiesberg. From Hebron we acquired 2 single-grain and 2 multigrain fractions of 4 grains each for low eU apatites from an amphibolite xenolith. Individual crystals were selected based on crystal form and clarity. Grains were examined for mineral inclusions using a binocular microscope with crossed polars. Dimensions were measured from photographed grains prior to packaging in Pt packets for analysis.

He measurements were made at the University of Colorado Boulder (CU) and the California Institute of Technology (Caltech). He analyses at Caltech followed the procedures outlined by House et. al. (2000). At CU, grains were heated at 6A for 5 minutes to extract the He gas. Extracted He was spiked with ^{3}He, purified using gettering methods, and analyzed on a quadrupole mass spectrometer. All degassed apatites were then retrieved, spiked with a ^{235}U-^{230}Th-^{145}Nd-^{51}V tracer, and dissolved in HNO_3 at ~90 °C for 1 hour. ^{238}U, ^{232}Th, ^{147}Sm and the tracer isotope analyses were acquired on an Agilent 7500 Series ICPMS for the apatites degassed at Caltech, and on a Thermo-Finnigan Element ICPMS at the University of California Santa Cruz for the apatites

degassed at CU. Masses were calculated using the grain dimensions. This dimensional mass was used to calculate the U and Th concentrations. Fragments of the Durango apatite were analyzed as a standard by the same procedures along with our samples. A hexagonal-prism geometry was used for the alpha-ejection correction (Farley et al., 1996). Analytical uncertainties for the individual analyses are based on propagated error from He, U, Th, and grain measurement uncertainties.

THERMAL HISTORY SIMULATIONS

Thermal history simulations were conducted using the inverse modeling capabilities of HeFTy, which simulates random time-temperature (tT) paths conforming to defined thermal history constraints and finds "good" and "acceptable" fit thermal histories that simultaneously satisfy the date, eU, and equivalent spherical radius (r) for each sample (Ketcham, 2005). The "good" fits are intended to be good to the limit of statistical precision, and defined such that the mean of goodness-of-fit statistics assessed is 0.5, and the minimum is 1/(N+1), where N is the number of statistics used (Ketcham et al., 2009). For each sample between 10,000 and 100,000 random tT paths were simulated to constrain the full range of "good-fit" histories. Each kimberlite was modeled individually using the RDAAM for apatite He retentivity (Flowers et al., 2009). For Melton Wold and Hebron, samples with a limited eU range and well-clustered AHe dates, the mean date, sample standard deviation, eU and r values were simulated. For Markt and Uintjiesberg, which show significant date-eU correlations, data were grouped into low-, mid- and high-eU bins and the average of each bin was modeled. The eU bins were <25 ppm, 25-50 ppm, 50-75 ppm, and >75 ppm, depending on the eU range of the

sample. The uncertainty for each bin was either the standard deviation within the bin, or 15% of the average AHe age for the bin for very tightly clustered bins.

Each model started at 120 °C at the time of kimberlite eruption and ended at present with the modern average surface temperature of 20°C. The emplacement dates used were published Rb/Sr mica and whole rock isochrons for Markt (116.8 ± 1.0 Ma, Smith et al., 1994), Uintjiesberg (100.7 ± 1.4 Ma, Smith et al., 1985), and Hebron (74.3 ± 0.6 Ma, also sometimes called Hartbeesfontein, Smith et al., 1994), and a U/Pb perovskite date for Melton Wold (143 ± 14 Ma, Smith et al., 1994). Simulations with these constraints make two assumptions: 1) the basement xenoliths either resided at temperatures and depths great enough for complete He loss and radiation damage annealing prior to eruption or were heated sufficiently by kimberlite entrainment to reset the He system and heal any radiation damage to the crystal, and 2) the published emplacement dates are accurate.

In the case of the Uintjiesberg kimberlite the highest eU grains have older AHe dates than the published emplacement age for the pipe, implying that one of these assumptions is not valid. This observation suggests that either the pipe is older than the published date, or that the high eU apatites were not fully reset during the eruption. We modeled both scenarios (Fig. DR1). In one we allowed the pipe emplacement date to be as old as 130 Ma (Fig. DR1a), and in the second we did not include the highest eU bin in the model (Fig. DR1b). Kimberlites can be tricky to date; for instance the published dates for Markt span 10 Ma from 116.8 ± 1.0 Ma (Smith et al., 1994) to 127 ± 3 Ma (Skinner et al., 1992), with both constrained by Rb/Sr isochrons. The U-Pb perovskite date for Melton Wold (143 ± 14) is imprecise, and nearby pipes with similar transitional chemical

affinities have been dated more precisely at 173 ± 1.9 (Droogfontein, Rb/Sr isochron, Smith et al., 1994). It is conceivable then that the emplacement date for Uintjiesberg is older than the published dates. However for Uintjiesberg, Rb/Sr isochrons (Smith et al., 1985), U/Pb zircon and zircon fission-track (Allsopp et al., 1989) dates appear to agree on an emplacement date of ~100 Ma. For this reason we favor the simulations excluding the high eU bin as not fully reset (Fig. 2c, Fig. DR1b). This has interesting implications for the eruption mechanisms of the kimberlite, but does not affect our main conclusions. Both models (Fig. DR1) still require cooling to 60 °C by 90 Ma and 10-20 °C of Tertiary cooling. The model allowing an older emplacement age (Fig DR1a) does imply earlier cooling than the model we have chosen to use (Fig. DR1b), but it does not change our major interpretations.

Two analyses for Markt are similarly older than the kimberlite emplacement age, fall off the date-eU correlation, and are excluded from the simulations. We suggest either that these apatites similarly suffered from incomplete He loss during entrainment, or were affected by He injection from neighboring high eU phases that would induce an anomalously old date and preferentially impact lower eU apatites.

UNROOFING ESTIMATES

We used two methods to estimate the magnitudes of material removed from the landscape: stratigraphic thickness estimates and conversion of the good-fit temperature envelopes from the tT models to depths. Mesozoic unroofing magnitudes were estimated by constructing the cross section in Figure 3 and using stratigraphic thickness estimates that are summarized in Hanson (2007). Karoo basin geometry was taken from the

1:1000000 structure map of South Africa (Visser, 1995), which contours the base of the basin. The stratigraphic thicknesses near Melton Wold are estimated at ~380m of Dwyka, ~1100m of Ecca, and >1850m of Beaufort (Winter and Venter, 1970). These thicknesses were extrapolated along the section using the isopach maps of Ryan (1968), and a combination of thinning rates and paleo-thicknesses (Johnson, 1976; Johnson, 1994; Johnson et al., 1996; Visser, 1972). We chose to use a N-S thinning rate of ~1 m/km for the Ecca Group, and ~10 m/km for the Beaufort Group. The published thinning rates for the Ecca group often include the Dwyka group, so we chose not to use a thinning rate for the Dwyka. These rates are in the range of published values and yield consistency with the mapped location of the contacts along section. The paleo-thickness of the Karoo basalts in this region is not known, but Hanson (2007) estimated it to be 700-1400m. For our model we chose to use a uniform thickness of 1000 m for the basalts. There is several hundred meters of uncertainty in the cumulative stratigraphic thicknesses of the model (Fig. 3). However, the reconstructions are internally consistent and honor the published thickness estimates, exposed contacts, basin geometries, and exposed kimberlite facies based on expected kimberlite geometry (Hawthorne, 1975).

Estimates of unroofing between 140 and 100 Ma are based dominantly on the type of basalt xenoliths contained within the studied pipes. The Karoo basalt remnant in Lesotho presently has a thickness of ~1800 m and the upper Lesotho Formation (~1200 m thick), is divided into units by chemical stratigraphy (Hanson et al., 2009; Marsh et al., 1997). The upper units (Monthae, Senqu, and Maloti) are presently ~800m thick, and are difficult to distinguish chemically, while the lower ~400m thick Mafika Lisiu unit is chemically distinguishable (Hanson et al., 2009). Markt (~117 Ma) and Melton Wold

(~143 Ma) contain xenoliths of the upper units, while Uintiesberg (~101 Ma) contains only the lower Mafika Lisiu unit. Markt also contains "evolved" xenoliths, for which there are several possible interpretations, but the favored one is that this evolved chemistry represents a unit higher in the stratigraphy that is no longer present in the Lesotho section (Hanson, 2007). If the thicknesses in our study area were the same as still preserved in Lesotho, this suggests >800m of erosion at Markt and up to 800 m of erosion at Melton Wold before the emplacement of Uintiesberg. However, the original thickness of basalt in this area is unknown, and likely to be less than that in Lesotho, so we suggest that 800 m is a maximum estimate for pre-100 Ma erosion.

We use this geologic information to more tightly constrain what we consider the most likely history for the region as depicted in the unroofing model (Fig. 3). For instance, thermal models for Melton Wold allow a significant amount of cooling between 140 Ma and 120 Ma, but while some erosion could have occurred at this time, the basalt xenoliths require the magnitude to be limited. Similarly, the basalt xenoliths in Uintjiesberg require significant exhumational cooling to denude the lowest basalt units and the upper Karoo sedimentary section that are no longer preserved at this location. Based on the amount of missing Karoo section and the thermal history models that imply most cooling occurred by 90 Ma, we suggest 1-1.5 km of erosion between ~100 Ma (when Uintjiesberg was emplaced) and 90 Ma. However, this estimate also has several hundred meters of uncertainty because it depends on the thickness estimates for the Karoo sequence and the thickness of basalt present when Uintjiesberg was emplaced.

Unroofing magnitudes for the Cenozoic erosional phase were based on paleodepth estimates from temperatures allowed by the "good-fit" paths in the inverse models. This

simple calculation evaluates the lowest and highest allowable temperatures at 45 Ma and converts these to a depth using a linear 20°C/km geothermal gradient and a 20°C average surface temperature, reasonable for this area of South Africa (Jones, 1988; Nyblade et al., 1990). For example, at 45 Ma tT paths require that the sample from Markt is at least as hot as 40 °C, but not hotter than 50 °C, which yields 1-1.5 km of unroofing. Similarly, Uintjiesberg must be between 30°C and 40 °C at 45 Ma, requiring 0.5-1 km of unroofing between then and the present. Hebron and Melton Wold are permitted to be as warm as 40 °C at 45 Ma, but can be at surface temperatures at that time, so they allow for up to 1 km of erosion, but do not require any erosion post-45 Ma.

REFERENCES CITED

Allsopp, H.L., Bristow, J.W., Smith, C.B., Brown, R., Gleadow, A.J.W., Kramers, J.D., and Garvie, O.G., 1989, A summary of radiometric dating methods applicable to kimberlites and related rocks, *in* Proceedings of the 4th International Kimberlite Conference, Volume 1: Perth, p. 343-357.

Farley, K.A., Wolf, R.A., and Silver, L.T., 1996, The effects of long alpha-stopping distances on (U-Th)/He ages: Geochimica Et Cosmochimica Acta, v. 60, p. 4223-4229.

Flowers, R.M., Ketcham, R.A., Shuster, D.L., and Farley, K.A., 2009, Apatite (U-Th)/He thermochronometry using a radiation damage accumulation and annealing model: Geochimica Et Cosmochimica Acta, v. 73, p. 2347-2365.

Hanson, E.K., 2007, Estimating erosion of Cretaceous-aged kimberlites in the Republic of South Africa through the examination of upper-crustal xenoliths [M.Sc. Thesis]: Grahmstown, South Africa, Rhodes University, 147 p.

Hawthorne, J.B., 1975, Model of a kimberlite pipe: Physics and Chemistry of the Earth, v. 9, p. 1-15.

House, M.A., Farley, K.A., and Stockli, D., 2000, Helium chronometry of apatite and titanite using Nd-YAG laser heating: Earth and Planetary Science Letters, v. 183, p. 365-368.

Johnson, M.R., 1976, Statigraphy and sedimentology of the Cape and Karoo sequences in the Eastern Cape Province [Ph.D. Thesis]: Grahmstwon, South Africa, Rhodes University, 276 p.

Johnson, editor, 1994, The Lexicon of South African Stratigraphy Part 1: Phanerozoic Units., Geological Survey of South Africa Handbook, 56 p.

Johnson, M.R., Van Vuuren, C.J., Hegenberger, W.F., Key, R., and Shoko, U., 1996, Stratigraphy of the Karoo Supergroup in southern Africa: an overview: Journal of African Earth Sciences, v. 23, p. 3-15.

Jones, M.Q.W., 1988, Heat flow in the Witwatersrand Basin and environs and its significance for the South African shield geotherm and lithosphere thickness: Journal of Geophysical Research: Solid Earth, v. 93, p. 3243-3260.

Ketcham, R.A., 2005, Forward and inverse modeling of low-temperature thermochronometry data, in Reiners, P.W., and Ehlers, T.A., eds., Low-Temperature Thermochronology: Techniques, Interpretations, and Applications: Mineralogical Society of America Reviews in Mineralogy and Geochemistry, Volume 58, p. 275-314.

Ketcham, R.A., Donelick, R.A., Balestrieri, M.L., and Zattin, M., 2009, Reproducibility of apatite fission-track length data and thermal history reconstruction: Earth and Planetary Science Letters, v. 284, p. 504-515.

Marsh, J.S., Hopper, P.R., Rehacek, J., Duncan, A.R., 1997, Stratigraphy and age of Karoo basalts aof Lesotho and implications for correlations within the Karoo Igneous Province. *In:* J.J. Mahoney and M.F. Coffin, editors, Large Igneous Provinces: Continental, Oceanic and Planetary Flood Volcanism. Geophysical Monograph 100. American Geophysical Union. Washington DC, p. 247-272.S

Nyblade, A.A., Pollack, H.N., Jones, D.L., Podmore, F., and Mushayandebvu, M., 1990, Terrestrial heat flow in east and southern Africa: Journal of Geophysical Research: Solid Earth, v. 95, p. 17371-17384.

Ryan, P.J., 1968, Stratigraphic and Paleocurrent Analysis of the Ecca Series and Lowemost Beaufort Beds in the Karoo Basin of South Africa [Ph.D. Thesis]: Johannesburg, South Africa, University of the Witwatersrand, 210 p.

Skinner, E.M.W., Smith, C.B., Viljoen, K.S., and Clark, T.C., 1992, The petrography, tectonic setting and emplacement ages of kimberlites in the south western border region of the Kaapvaal Craton, Prieska area, South Africa, *in* Proceedings of the 5th International Kimberlite Conference, Volume 1, p. 80-97.

Smith, C.B., Allsopp, H.L., Kramers, J.D., Hutchinson, G., and Roddick, J.C., 1985, Emplacement ages of Jurasic-Cretaceous kimberlites byt the Rb-Sr method on phlogopite and whole rock samples: Transactions of the Geological Society of South Africa, v. 88, p. 249-266.

Smith, C.B., Clark, T.C., Barton, E.S., and Bristow, J.W., 1994, Emplacement Ages of Kimberlite Occurrences in the Prieska Region, Southwest Border of the Kaapvaal Craton, South-Africa: Chemical Geology, v. 113, p. 149-169.

Visser, D.J.L., 1972, Sedimentere insluitsels van Karoo-ouderdom in kimberliet can die Finsche-diamantmyn: Tyskrif vir Natuurwetenskappe, p. 32-36.

Visser, 1995, Structure map of the Republic of South Africa and the kingdoms of Lesotho and Swaziland: Council for Geoscience, South Africa, scale 1:1 000 000, 4 sheets.

Winter, H.d.l.R., and Venter, J.J., 1970, Lithostratigraphic correlations of recent deep boreholes in the Karoo-Cape sequence, *in* Haughton, S.H., ed., 2nd IUGS Symposium on Gondwana Stratigraphy and Paleontology: Pretoria, South Africa, p. 395-408.

Stanley et. al. Figure DR1

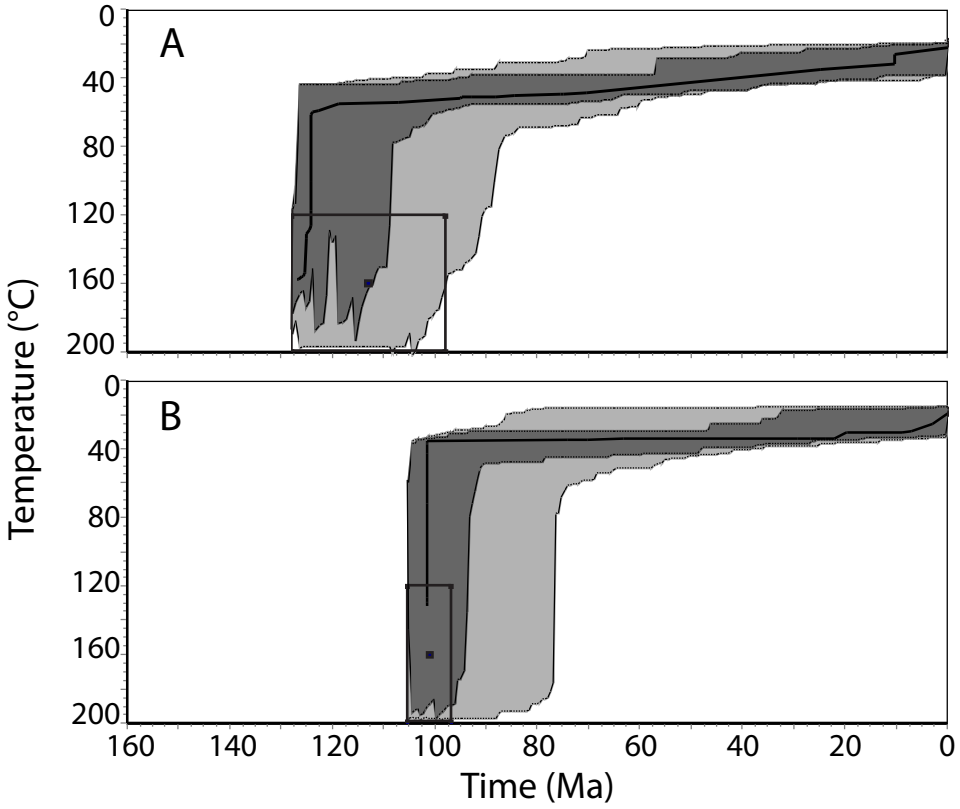

Figure DR1. Alternate thermal history simulations for the Uintjiesberg kimberlite. Dark grey fields are the envelopes of good-fit paths, light grey are acceptable fits. Black line is the best fit path, and black boxes indicate model constraints. A) Simulation includes all data and allows kimberlite emplacement as early as 130 Ma. B) Simulation excludes the highest eU bin based on the assumption that it is not fully reset (same as Fig. 2E).

Table DR1. Apatite (U-Th)/He data from select kimberlites, Prieska region, South Africa

Sample	Mass (ug)	Grains	l[a] (um)	r[a] (um)	Ft[b]	U (ppm)	Th (ppm)	eU[c] (ppm)	Sm (ppm)	He (nmol/g)	Raw date (Ma)	Corr date (Ma)	1σ[d] (Ma)
SA11-33A: Melton Wold Kimberlite													
a1	2.6	1	176	43	0.70	5.1	10.5	7.6	68.8	3.8	58	82	3.5
a2	1.7	1	131	40	0.66	6.6	25.9	12.7	84.6	5.3	60	91	3.9
a3	5.4	1	177	61	0.77	6.9	19.9	11.6	66.2	5.0	67	86	2.8
SA11-57A: Markt Kimberlite													
a1	2.3	1	179	49	0.69	8.7	0.0	8.7	1.7	4.4	91	131	0.5
a2	2.5	1	156	52	0.69	10.9	0.0	10.9	0.9	2.2	35	50	0.2
a3	1.1	1	137	39	0.59	8.4	0.0	8.4	1.8	1.0	22	36	0.1
a4	2.6	1	131	54	0.73	10.5	0.0	10.5	1.3	2.7	45	63	0.3
a5	1.5	1	132	44	0.66	16.0	0.0	16.0	1.9	2.7	31	47	0.2
SA11-57B: Martk basement xenoliths													
a1	7.3	1	164	75	0.81	70.4	24.5	76.1	15.7	35.6	70	87	2.0
a2	7.2	1	160	75	0.80	32.3	22.7	37.6	98.4	19.9	79	99	2.4
a3	8.3	1	130	89	0.82	21.2	7.7	23.0	16.7	15.1	62	75	1.9
a4	7.4	1	147	79	0.81	37.9	37.2	46.7	125.2	33.1	83	102	2.6
a5	3.1	1	138	53	0.74	24.6	20.6	29.5	124.9	24.3	93	126	3.7
SA11-27C: Uinjiesberg basement xenoliths													
a1	1.0	1	98	39	0.63	97.1	40.5	106.6	1.5	51.0	73	139	0.7
a2	1.7	1	143	46	0.65	57.5	7.2	59.1	0.9	26.5	68	121	0.7
a3	1.2	1	104	41	0.65	63.5	0.0	63.5	1.6	22.6	56	99	0.5
a4	2.0	1	113	50	0.71	60.5	0.0	60.5	0.8	22.8	60	96	0.6
a5	2.2	1	142	50	0.70	102.6	59.4	116.5	0.7	54.9	79	121	1.1
SA11-27D: Uintjiesberg kimberlite													
a2	36.1	1	256	132	0.88	0.1	1.3	0.5	10.8	0.4	63	72	3.1
a4	10.0	1	168	86	0.82	0.2	1.0	0.4	10.9	0.2	63	77	6.4
SA11-56B: Hebron amphibolite xenolith													
a1	14.6	1	270	82	0.82	1.1	17.3	5.2	32.0	1.7	42	52	1.6
a5	7.9	1	189	72	0.77	0.3	14.4	3.6	169.6	1.8	58	75	3.0
ma1	18.1	4	170	61	0.75	0.9	13.9	4.2	6.6	1.2	54	72	0.7
ma2	19.8	4	140	65	0.78	0.1	0.6	0.2	7.6	0.1	63	80	0.6

[a] l - length, r - radius

[b]Ft is alpha-ejection correction of Farley et al (1996).

[c]eU - effective uranium concentration, weights U and Th for their alpha productivity, computed as [U] + 0.235 * [Th]

[d]Analytical uncertainty based on U, Th, He, and grain length measurements